

Endostitch automation using 2D and 3D vision.

Kasper Claes¹ and Herman Bruyninckx¹

Department of Mechanical Engineering, Katholieke Universiteit Leuven,
Celestijnenlaan 300B, 3001 Leuven (Heverlee), Belgium,
{first.last}@mech.kuleuven.be

Abstract. This paper describes the automation of a surgical instrument called the Endostitch. The Endostitch is a manual tool for laparoscopic suturing. Laparoscopy refers to endoscopic operations within the abdomen. We automated this tool and control it using a digital I/O card in a PC.

The goal of our research is to automate suturing after specific laparoscopic procedures using the automated Endostitch mounted on a robotic arm. To this end a partial 3D scan of a (mockup for an) organ is acquired using structured light. 2D and 3D vision algorithms are combined to track the location of the tissue to be sutured.

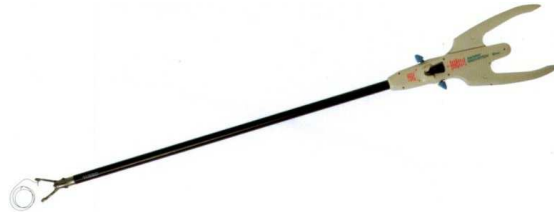
1 Introduction

This work attempts to progress into robotic control using structured light scanning with a projector and a camera. The application we chose is (semi)automatic suturing for certain operations in laparoscopy. These operations usually only make four incisions of a few mm: two for surgical in-

struments, one for the endoscope and one for insufflating CO_2 -gas in order to give the surgeon some work space. These incisions are a lot smaller than the incision that is made for open surgery, which is typically 20cm long. The advantages are clear: less blood loss, faster recovery, less scar tissue and less pain (although the effects of the gas can also be painful after the operation).

However, performing these operations requires specific training, they are more difficult since the instruments make constraintuitive movements: e.g. moving one end of the instrument to the left moves the other to the right, as the instruments have to be moved around an invariant point. The velocity of the tool tip is also scaled depending on the ratio of the part of the instrument out and inside the body at every moment. This can amplify the surgeon's tremor. Also the surgeon has reduced sight and haptic feedback.

Suturing at the end of an endoscopic operation is a time demanding and repetitive job. The faster it can be done the shorter the operation, and the faster the patient can recover. Moreover, robotic arms are more precise than the slightly trembling hand of the surgeon. Therefore, it seems useful to research (semi)automate



suturing.

Displaying a 3D reconstruction of the organs eases the task of the surgeon since the depth cannot be guessed from only video images. Another reason for calculating the field of view in three dimensions is its need for estimating the motion of the organ (and then compensating for it), or extracting useful features. There are several approaches possible for measuring the depth:

Stereo endoscopes have two optical channels and thus have a larger diameter than normal endoscopes. Therefore often not used in practice, other types of 3D vision need to be explored for this application:

Thormählen ([1]) presented a system for three-dimensional endoscopy using optical flow, with a reconstruction of the 3D surface of the organ. For this research he only used the video sequences of endoscopic surgery (no active illumination). Others use laser to actively illuminate the scene, like Hayashibe ([2]) who inserts an extra instrument into the abdomen with a laser. That laser scans the surface using a galvano scanner with two mirrors, and triangulation between the endoscope and the laser yields a partial 3D reconstruction of the organ.

The group of de Mathelin also inserts such an extra laser instrument: Krupa ([3]) uses a tool that has three LEDs on it and projects four laser spots onto the organ. This limited structured light method enables them to keep calculations light enough to do visual servoing at high frequencies (in casu e.g. at 500Hz), and allows to accurately estimate repetitive organ motions, as for example published by Ginhoux ([4]).

This paper is organized as follows: section 2 elaborates on the automation of the Endostitch and section 3 discusses the work that has been done on the robotic arm motion control. Section 4 gives an overview of the structured light scanning, section 5 explains the combined 2D and 3D vision algorithms and section 6 is about future work.

2 Endostitch automation

An Endostitch is a suturing tool developed by Auto Suture in 2003 that decreases the operative time for internal suturing



during laparoscopic surgery. It has two jaws, a tiny needle is held in one jaw and can be passed to the other jaw by closing the handles and flipping the toggle levers. It is mainly used for treating hernias and in urology.

This tool was automated pneumatically with a rotative cylinder around the toggle levers and a linear one for the handles. Both cylinders have two end position interrogation sensors at either end of their range. Those sensors are electric proximity switches that output a different voltage whether or not they are activated. We connect those signals to the inputs of a digital I/O card. The state the Endostitch is in can thus be read in software.

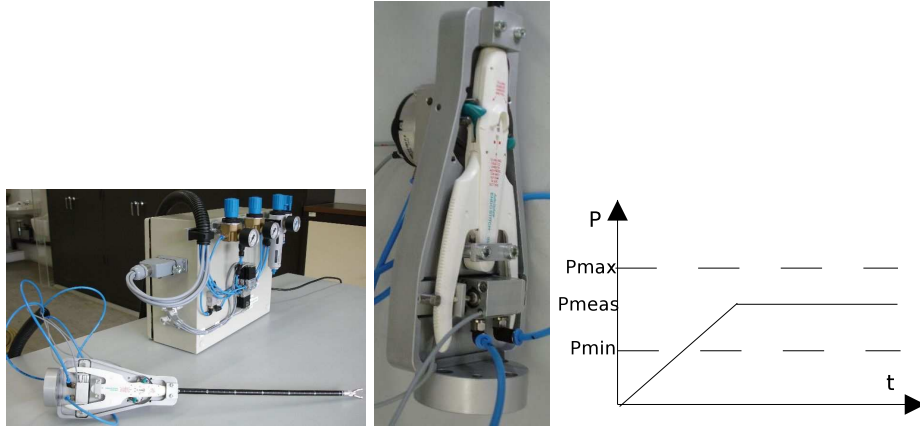


Fig. 1. Left: Pneumatically actuated Endostitch, right: 2 pressures possible

The pneumatic cylinders are actuated using TTL logic on the same card. We made use of the scripting language of our robot control software to implement a program that stitches any soft material, it functions at $2Hz$ now (a standard C++ interface is also provided). It was implemented as a state machine, see figure 2. The state each of the cylinders is triple: actuated in either direction or not actuated.

The local quality of human tissue determines whether it will hold or might tear when stressed after the operation. Therefore it is important to stitch using the stronger parts of the tissue.

When trying to close the jaws with tissue in between, the pressure could be increased linearly until the needle is able to pass through. That minimal pressure needed (P_{meas}) is a relevant cue to the quality of the tissue, and hence to whether or not that spot is suitable for the next stitch.

Experiments are being done to identify a minimal pressure P_{min} below which the tissue is not considered to be strong enough, and a maximal pressure P_{max} above which the tissue is probably of a different type. If the pressure needed to penetrate the tissue is in between those two, the stitch can be made at that location, see figure 1.

However, since it's only important that $P_{min} \leq P_{meas} \leq P_{max}$, then it is faster only to use the 2 discrete pressures P_{min} and P_{max} instead of continuously increasing the pressure. First try the tissue using P_{min} , if it passes through the tissue, the tissue is not strong enough. If it doesn't pass through the tissue, try again using P_{max} . If it passes this time, the tissue is suitable, otherwise try another spot.

As can be seen in figure 1, the case of the pneumatic actuation has three adjustable valves (in blue on top), that is one master valve that can decrease

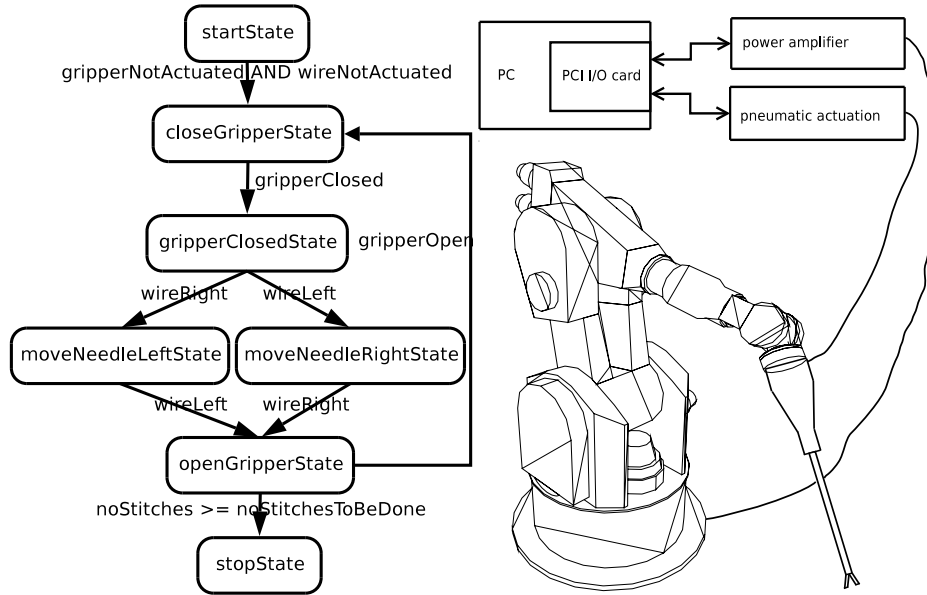


Fig. 2. Left: State machine, right: Setup with robot and Endostitch

the incoming pressure, and two valves for further reduction to P_{min} and P_{max} . Switching between P_{min} and P_{max} can be done in software.

3 Robotic arm control

The automated Endostitch is mounted onto a robotic arm as schematically illustrated in figure 2. Visual servoing of that robotic arm based on structured light ranging is work in progress. We have already done visual servoing experiments using a Krypton K600 CMM: a commercially available vision system which tracks LEDs using three line cameras, and calculates the 6D position of an object when multiple LEDs are used.

One robotic arm holds the mockup for the abdomen, see figure 3. It has a hole in it, simulating the trocar point. A 3D mouse moves this mockup in 3D, simulating the motion of the patient (e.g. of respiration). LEDs are attached to the mockup enabling the vision system to track it. The other robotic arm makes the gripper of the Endostitch move along a line (e.g. an artery) inside our 'abdomen' while not touching the edges of the trocar and compensating for the motion of the 'patient'. The robotic arm has six degrees of freedom, which are reduced to four in this application, since the trocar point remains constant.

We are replacing this vision system with our structured light system for two reasons. First, this structured light setup uses only consumer grade hardware (a projector and a camera) and is thus much less expensive. Furthermore, attaching LEDs is clinically difficult and we cannot assume the rest of the observed body to be statically attached to it: tracking of deformable structures is required.

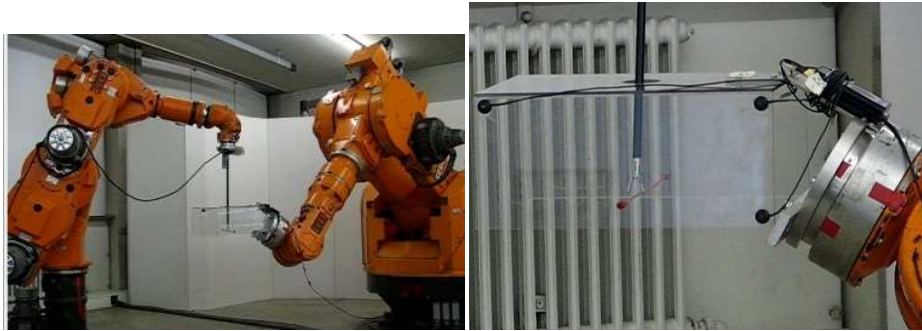


Fig. 3. Left: 2 Kuka robots cooperating on minimally invasive surgery mockup, right: Closeup with three LEDs

4 3D reconstruction using structured light



Fig. 4. Setup with camera, projector, calibration box and mockup

The type of structured light we are referring to uses a LCD projector that projects stripe patterns. In laparoscopy the structured light needs to be guided through the endoscope. The percentage of the light that is lost in doing so is considerable. Armbruster et al ([5]) for example built a prototype whose light intensity in the abdomen is sufficient in 1997. We do not have such a prototype in our lab yet, therefore the first experiments were conducted using a standard IIDC-compliant Firewire camera, see figure 4.

We use two structured light algorithms: one with standard sequences of binary patterns, and one that produces single frame reconstructions based on a static pattern. The former can only be used for static scenes since it needs multiple frames for one reconstruction. The latter can be used online producing reconstructions at a few Hz. (e.g. a 1.6GHz Pentium M with ATI M10 3D acceleration outputs 3 reconstructions a second). It is however less accurate than the other technique. Details can be found in [6].

The mockup is a semiplanar surface with a cut of a few cm made of a soft synthetic rubber of 2mm thick. Because the objects observed are small and

nearby we use a camera with zooming capabilities and exchanged the standard projector lens for a zoom lens. Figure 5 shows the results. The rougher dynamical meshes produced contain information about the state the suturing is in several times a second.

Organs cause specular reflection. On these highlights the camera normally oversaturates, for which we compensate in software based on a crude estimation of scene geometry. In previous work ([7]) we demonstrated the improvement using these compensations on a shiny metal object. This adapted structured light is explained further in [8].

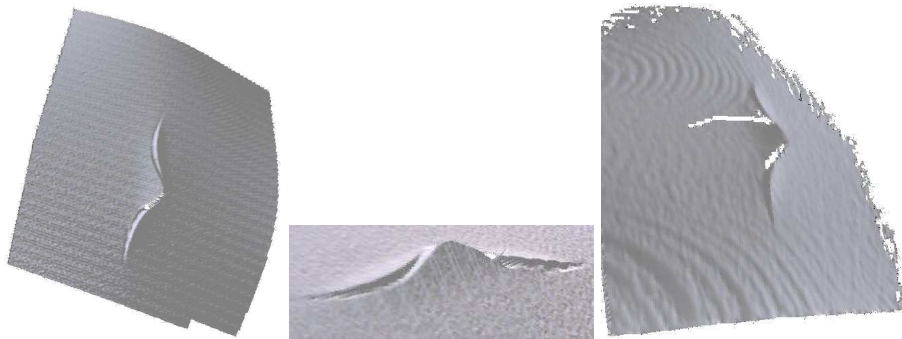


Fig. 5. Left to right: reconstruction for static scene, close-up, reconstruction using the single shot mode

5 Experiments: 2D and 3D vision combined

We use several visual cues based on the same images to enhance the robustness of tracking of the incision edges, 2D and 3D.

On the 2D image we use a snake algorithm as used by A.Blake (see [9]). The surgeon uses a mouse to roughly indicate a few points of the part to be sutured. A spline is fitted through these points and an edges are detected along line segments perpendicular to the knot points indicated. We use a 1D exponential filter to detect intensity edges bigger than a certain treshold: it is the ISEF filter by Shen and Castan (see [10]), see the white dots in figure 6 on the left.

The 2D knot pixels are used as texture coordinates to fit a 3D spline through the corresponding mesh points. A similar active contour algorithm is used, now in 3D: the edges are searched in the intersection between the mesh and a filled circle around the knot point perpendicular to the spline, see figure 7 on the left. An example of actual intersection data can be seen in figure 6 on the right. The data can be locally noisy (small local maxima), and outliers can occur, especially when using the rougher dynamical scans, which is necessary for visual servoing. This can be seen in figure 7 on the right. Therefore, the robustness of the method to extract the two maxima is important. We choose for an Expectation-Maximization approximation (see A.Dempster in [11]).

Inverse transform sampling (see e.g. [12]) is applied to the 1D signals in figures 6 and 7 on the right, because we need the pixel values on the x axis, not the height

values on the y axis. EM can be used here since we know that we are looking for two peaks. Having a reasonable estimate of the initial values of the peaks is necessary as EM is sensitive to the initial top values. We choose one to be the maximum of the intersection and the other one symmetrical around the center of the intersection, as indicated by the vertical lines in figure 6 on the right.

The online version of the system needs to be time efficient. Only the line segments (for the 2D image) or circles perpendicular (for the 3D mesh) to the spline are searched. The data are 1D intensity values for the former case, and 1D height values in the latter case. Within this drastically reduced search spaces, we use efficient algorithms: the ISEF filter is $O(N)$ where N is the number of intensity values in the line segment. Inversion sampling is also $O(N)$ where N is the number of height values in the mesh intersection. The EM algorithm is iterative but 5 iterations are sufficient for a reasonable convergence, its complexity is $O(I.C.N)$ where I is the number of iterations, C is the number of classes and N the number of height values in the intersection, hence in this case $10.O(N)$: also linear.



Fig. 6. Results in 2D and 3D for statical reconstruction (binary projection pattern sequence)

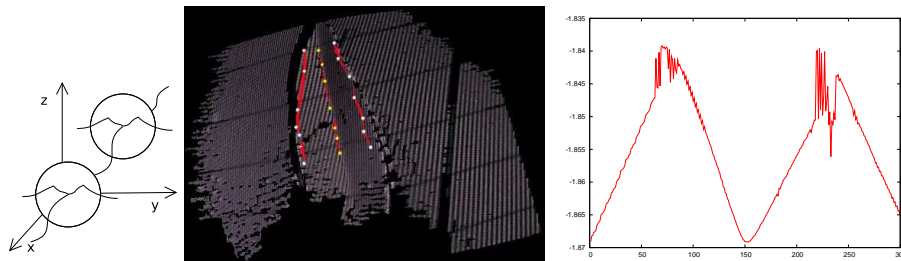


Fig. 7. Left: 3D data interpretation, middle: results in 3D for dynamical reconstruction (statical projection pattern), right: one of the corresponding intersections.

6 Future work

First we want to test these methods on actual organs. Bayesian estimation using the vision methods presented is being implemented. A voting scheme based on the 2D and 3D estimation will track more robustly. Other 2D (or 3D) cues will be added to it based on the same data. The online version will work with the dynamic scans and close the visual servoing loop. Path planning for the actual suturing process also needs to be implemented.

7 Conclusion

This paper presents the pneumatic automation of a manual suturing tool. The tool is attached to a robotic arm of which the motion is the sum of the desired motion for the surgical procedure and a motion compensation of (a mockup of) the patients abdomen. To track the deformable incision in the organ we use a combination of 2D (2D snakes using ISEF edge detection) and 3D vision (3D snakes using EM for robust geometry estimation).

Acknowledgment

The author would like to thank T.P.Koninckx for his structured light software, the Optidrive company for the pneumatical components and J.Rutgeerts for the control of the robot arm.

References

1. Thormaehlen, T., Broszio, H., Meier, P.: Three-dimensional endoscopy (2002)
2. Hayashibe, M., Nakamura, Y.: Laser-pointing endoscope system for intra-operative 3d geometric registration. Proceedings of the 2001 IEEE International Conference on Robotics and Automation (2001)
3. Krupa, A., Doigon, C., Gangloff, J., de Mathelin, M.: Combined image-based and depth visual servoing applied to robotized laparoscopic surgery. Proc. IEEE/RSJ International Conference on Intelligent Robots and Systems (2002)
4. Ginhoux, R., Gangloff, J., de Mathelin, M., Soler, L., Leroy, J.: A 500hz predictive visual servoing scheme to mechanically filter complex repetitive organ motions in robotized surgery. Proc. IEEE/RSJ Int.Conf. on Int.Robots and Syst. (2003)
5. Armbruster, K., Scheffler, M.: Messendes 3d-endoskop. *Horizonte* **12** (1998) 15–6
6. T.P.Koninckx, A.Griesser, Gool, L.: Real-time range scanning of deformable surfaces by adaptively coded structured light. Proc. IEEE 4th Int. Conf. on 3-D Digital Imaging and Modeling-3DIM03 (2003) 293–300
7. Anonymous: no title (2005)
8. T.P.Koninckx, P.Peers, P.Dutre, Gool, L.: Scene-adapted structured light. Proc. IEEE Int. Conf. on Computer Vision and Pattern Recognition-CVPR05 (2005)
9. Blake, A., Isard, M.: *Active Contours*. Springer, Berlin, Germany (1998)
10. Shen, J., Castan, S.: An optimal linear operator for step edge detection. *Computer vision, graphics & image proc.: graph.models & underst.* **54**, no.2 (1992) 112–133
11. Dempster, A.P., Laird, N.M., Rubin, D.B.: Maximum likelihood from incomplete data via the EM algorithm (with discussion). *Journal of the Royal Statistical Society (Series B)* **39** (1977) 1–38
12. Devroye, L.: *Non-Uniform Random Variate Generation*. Springer-Verlag, New York (1985)